Carbohydrate Polymers 131 (2015) 407–414

Contents lists available at ScienceDirect

Carbohydrate Polymers

journal homepage: www.elsevier.com/locate/carbpol

Alginate–hyaluronan composite hydrogels accelerate wound healing process

O. Catanzano[a], V. D'Esposito[b], S. Acierno[c], M.R. Ambrosio[b], C. De Caro[a], C. Avagliano[a], P. Russo[d], R. Russo[a], A. Miro[a], F. Ungaro[a], A. Calignano[a], P. Formisano[b], F. Quaglia[a,*]

[a] Department of Pharmacy, University of Naples Federico II, Via D. Montesano 49, 80131 Naples, Italy
[b] Department of Translational Medical Sciences, University of Naples Federico II, Via S. Pansini 5, 80131 Naples, Italy
[c] Department of Engineering, University of Sannio, Piazza Roma 21, 82100 Benevento, Italy
[d] Institute for Polymers, Composites and Biomaterials, National Research Council, Via Campi Flegrei 34, 80078 Pozzuoli (NA), Italy

ARTICLE INFO

Article history:
Received 7 February 2015
Received in revised form 14 May 2015
Accepted 15 May 2015
Available online 16 June 2015

Keywords:
Alginate
Hyaluronan
Internal gelation
Wound dressing

ABSTRACT

In this paper we propose polysaccharide hydrogels combining alginate (ALG) and hyaluronan (HA) as biofunctional platform for dermal wound repair. Hydrogels produced by internal gelation were homogeneous and easy to handle. Rheological evaluation of gelation kinetics of ALG/HA mixtures at different ratios allowed understanding the HA effect on ALG cross-linking process. Disk-shaped hydrogels, at different ALG/HA ratio, were characterized for morphology, homogeneity and mechanical properties. Results suggest that, although the presence of HA does significantly slow down gelation kinetics, the concentration of cross-links reached at the end of gelation is scarcely affected. The *in vitro* activity of ALG/HA dressings was tested on adipose derived multipotent adult stem cells (Ad-MSC) and an immortalized keratinocyte cell line (HaCaT). Hydrogels did not interfere with cell viability in both cells lines, but significantly promoted gap closure in a scratch assay at early (1 day) and late (5 days) stages as compared to hydrogels made of ALG alone ($p < 0.01$ and 0.001 for Ad-MSC and HaCaT, respectively). *In vivo* wound healing studies, conducted on a rat model of excised wound indicated that after 5 days ALG/HA hydrogels significantly promoted wound closure as compared to ALG ones ($p < 0.001$). Overall results demonstrate that the integration of HA in a physically cross-linked ALG hydrogel can be a versatile strategy to promote wound healing that can be easily translated in a clinical setting.

1. Introduction

Wound repair is one of the most complex biological processes consisting in the activation of numerous intracellular and intercellular pathways able to restore tissue integrity and homeostasis (Gurtner, Werner, Barrandon, & Longaker, 2008). Dressings have been applied to open wounds for centuries to prevent further injury and bacterial invasion, but nowadays their design has evolved toward multifunctionality to better control potential infections and to aid the healing process (Queen, Orsted, Sanada, & Sussman, 2004). A key property of modern dressings is their ability to retain and to create a moist environment around the wound facilitating healing. To this purpose a number of new materials have been developed and tested. Amid modern dressings, hydrogels cover a large segment due to their well-recognized biocompatibility (Boateng, Matthews, Stevens, & Eccleston, 2008) and the capacity to absorb the exuding liquids and debris from the wound area. Furthermore, hydrogels are typically soft and elastic above their glass transition temperature due to their thermodynamic compatibility with water (Peppas, Huang, Torres-Lugo, Ward, & Zhang, 2000; Slaughter, Khurshid, Fisher, Khademhosseini, & Peppas, 2009). Hydrogels are currently employed in several biomedical applications where they act as a three-dimensional scaffold for tissue engineering or as a water-controlled platform for drug delivery (Lee & Mooney, 2012).

Alginates (ALGs) are linear blocks copolymers composed of 1-4-linked β-D-mannuronic acid (M) and α-L-guluronic acid (G) forming G- or M-blocks, or alternating M and G sequences of different length. Due to their biocompatibility and bioresorption properties, ALGs have been widely used in regenerative medicine (Slaughter et al., 2009) and successfully applied to treat a wide variety of secreting lesions. Indeed, their high water absorption limits wound secretions and minimizes bacterial contamination (Gilchrist & Martin, 1983). Furthermore, ALG dressings maintain

* Corresponding author. Tel.: +39 81 678707; fax: +39 81 678707.
E-mail address: Quaglia@unina.it (F. Quaglia).

http://dx.doi.org/10.1016/j.carbpol.2015.05.081
0144-8617/

a physiologically moist microenvironment that promotes healing and formation of granulation tissue. ALGs can be rinsed away from wound bed with saline irrigation, so that the removal of the dressing does not alter the neo-formed granulation tissue and is virtually painless. Another important aspect of ALG dressing is related to management of wound exudate, allowing significant limitation of maceration phenomena at wound periphery. ALG dressings can be designed to absorb large volumes of exudate, whilst continuing to provide a moist wound environment. ALG-based absorbent wound dressing may be used on multiple wound types, including but not limited to diabetic wounds, venous wounds, pressure ulcers, cavity wounds, and some bleeding wounds.

A well-established key requirement to apply hydrogels in the biomedical field consists in a full control of material properties. Covalent crosslinking is an elective way to stabilize three dimensional polymer networks for a variety of applications. However, chemical crosslinking reagents can show severe toxicity resulting in limited application in the biomedical field. Ionically cross-linked ALG hydrogels are produced taking advantage of their propensity to coordinate several divalent cations such as Ca^{2+}, Ba^{2+}, Sr^{2+}, Zn^{2+}, Cu^{2+}, Cd^{2+}, and Co^{2+} (Morch, Donati, Strand, & Skjak-Braek, 2006). Divalent cations allow ionic interactions between G-rich regions of adjacent polymer chains resulting in the formation of a bulk structure in a shape of an 'egg-box' (Braccini & Perez, 2001; Grant, Morris, Rees, Smith, & Thom, 1973). Addition of soluble calcium salts to an ALG solution has been largely applied to produce ALG hydrogels although rapid and inadequately controlled gelation process leads to formation of hydrogels with scarce structural homogeneity and poor mechanical properties (Kuo & Ma, 2008; Skjåk-Bræk, Grasdalen, & Smidsrød, 1989). To overcome this drawback, internal gelation of ALG through $CaCO_3$–GDL (D-glucono-δ-lactone) system providing slow release of calcium ions has been proposed as a versatile and straightforward strategy to obtain homogenously cross-linked hydrogels. The kinetics of ALG gelation process has been studied extensively (Draget, Ostgaard, & Smidsrod, 1990; Draget, Ostgaard, & Smidsrod, 1989; Draget et al., 1993) and the final properties of the hydrogels proved to be affected by the M/G ratio, alginate concentration, and particle size of the calcium salts.

Hyaluronan (HA) is a nonsulfated, linear glycosaminoglycan, consisting in repeating units of (β,1-4)-D-glucuronic acid and (β,1-3)-N-acetyl-D-glucosamine. High molecular weight HA (>100 kDa) is present in most living tissues and in large amounts in the skin (dermis and epidermis), brain and central nervous system (Toole, 2004) constituting the most relevant structural element of extracellular matrix. HA role as regulator of tissue hydrodynamics, comprising cell dynamics, inflammation and tissue repair has strongly emerged in the last few years pointing at its application in several pathological situations (Petrey & de la Motte, 2014). In the early stages of wound healing, HA provides a temporary support facilitating transport of nutrients and waste products while increasing keratinocyte migration and proliferation (Dicker et al., 2014). Due to its affinity with water, correct wound hydration is nonetheless ensured. Exogenous HA was found to accelerate skin wound healing in rats (Foschi et al., 1990), hamsters (King, Hickerson, & Proctor, 1991) and also diabetic foot ulcers, i.e. the most difficult lesions to treat among chronic wound (Frenkel, 2012; Voigt & Driver, 2012). Furthermore, HA and its related low molecular weight products modulate the expression of fibroblast genes involved in remodeling and repair of extracellular matrix (David-Raoudi et al., 2008) and play a role in the control of angiogenesis (West, Hampson, Arnold, & Kumar, 1985). HA may also protect granulation tissue from the deleterious effects of oxygen free radical due to its scavenging activity (Trabucchi et al., 2002).

In the present study, we propose an ALG/HA hydrogel with enhanced wound healing activity potentially useful as platform for wound dressing. Internal gelation technique was used for cross-linking ALG/HA solutions at different HA ratio, and the resulting disk-shaped hydrogels were fully characterized. The gelation dynamics was monitored through rheological measurements to evaluate the influence of HA on the cross-linking process. Biocompatibility and wound healing potential of ALG/HA were evaluated on different cell lines. Human adipose-derived mesenchymal stem cells (AdMSCs), a multipotent non-hematopoietic stem cell line, was selected due to overwhelming interest in cell therapy and tissue engineering (Kocaoemer, Kern, Kluter, & Bieback, 2007). Then, the migration of AdMSCs and human keratinocytes (HaCaT) in a scratch assay, a well-known systems modeling very closely the repairing process during re-epithelialization (Gurtner et al., 2008; Singer & Clark, 1999) was assessed. Finally, *in vivo* wound healing activity has been evaluated in a rat model of excised wound.

2. Materials and methods

2.1. Materials

Sodium alginate (ALG) (from *Macrocystis Pyrifera*, medium viscosity, 360 cps at 25 °C) was purchased from Farmalabor (Italy). Hyaluronan (HA) sodium salt from *Streptococcus equi* ($1.5–1.8 \times 10^6$ Da), calcium carbonate, calcium chloride dihydrate, sodium chloride, potassium chloride, sodium phosphate dibasic, D-glucono-δ-lactone (GDL) and all reagents used for sulforhodamine assay were obtained from Sigma–Aldrich (St. Louis, MO). Ethanol was purchased from Carlo Erba (Italy). Media, sera, and antibiotics for cell cultures were from Lonza (Lonza Group Ltd, Basel, Switzerland). Distilled water was used throughout this study.

2.2. ALG/HA hydrogel preparation

ALG hydrogels were prepared according the method of Kuo and Ma (2001). Briefly, ALG (1% w/v) was dissolved in deionized water and mixed with calcium carbonate to form a 30 mM suspension. A freshly prepared 64 mM GDL solution in water was then added to the suspension and vortex-mixed to initiate gelation. HA (10% or 20% of ALG weight) was dissolved directly in the ALG solution to give 10% (ALG/HA10) and a 20% (ALG/HA20) w/w hydrogels. Solutions were cast in 96-well culture plate (50 μL) or in 24-well culture plate (1 mL) to form circular disks either 2 mm in thickness and 5 mm in diameter or 5 mm in thickness and 15 mm in diameter, respectively. The well plates were capped, sealed with Parafilm®, and gelled on a horizontal surface at room temperature for 24 h. After gelation the ALG disks were washed with water and stored at 4 °C.

2.3. Hydrogel characterization

The bulk morphology of the ALG/HA hydrogels was analyzed through scanning electron microscopy (SEM). First the hydrogels were frozen overnight at −20 °C, and lyophilized at 0.01 atm in a Modulyo apparatus (Edwards, UK). Then the samples were stuck on a metal stub and coated with gold under vacuum for 90–120 s. Images were obtained using Quanta 200 FEG (FEI, USA).

Gelation time and viscoelastic properties of gels were measured using a strain-controlled rotational rheometer (ARES, Rheometric Scientific Inc., USA) equipped with a dual-range force rebalance transducer (2KFRT). Measurements were performed using 25 mm parallel plates geometry and maintaining the samples at 22 °C.

Homogeneity of the ALG hydrogels was evaluated by measuring the dry/wet weight ratio. Gels were cut perpendicular to the cylinder axis into 4 slices with approximately the same thickness. Each slice was weighted, dried at 45 °C for 48 h and weighted again.

Cross-linking degree of the ALG hydrogels was evaluated by soaking the hydrogel disk in 15 mL of a 1, 3 or 5 mM calcium

chloride solution at 37 °C under gentle shaking. The external medium was replaced every day. At scheduled time, the specimens were withdrawn, quickly blotted twice on a filter paper and weighted. The swelling ratio W/W_0 was calculated from the ratio between wet weight at designated time (W) and initial wet weight (W_0).

2.4. Cell lines

Mesenchymal Stem Cells (Ad-MSCs) were isolated from human adipose tissue biopsies as previously described (D'Esposito et al., 2012). Cells were cultured at 37 °C with Dulbecco's modified Eagle's medium (DMEM) and Ham's F12 (1:1) with 10% Fetal Bovine Serum (FBS), 2 mM glutamine, 100 IU/mL penicillin, and 100 IU/ml streptomycin. Cultures were maintained in humidified atmosphere of 95% air and 5% CO_2 at 37 °C.

Immortalized keratinocyte cell line HaCaT (CRL2309) was obtained from American Type Culture Collection (Manassas, VA, USA). HaCaT were cultured in DMEM containing 10% FBS, penicillin/streptomycin (10,000 U/mL), L-glutamine (2 mM) and placed in a humidified incubator under of 95% air and 5% CO_2 at 37 °C. Cells were passaged at confluence using a solution of 0.5% trypsin and 0.2% EDTA.

2.5. In vitro *toxicity and scratch assay on Ad-MSCs and HaCaT*

Ad-MSC viability was assessed using 24-transwell culture system (0.4-μm pore polycarbonate membranes) (Costar, Cambridge, MA). Cells were loaded at 50,000 cells per insert in the lower chamber. The following day, the hydrogels were added to the upper chamber in complete medium. Upon 24 h, sulforhodamine assay was used to evaluate their viability (Chiba, Kawakami, & Tohyama, 1998). Briefly, the upper chamber was removed and the cells were fixed with 50% trichloroacetic acid for at least 2 h at 4 °C. Then, cells were washed 5 times with distilled and de-ionized water. After air-drying, cells were stained for 30 min with 0.4% sulforhodamine dissolved in 1% acetic acid. Unbound dye was removed by five washes with 1% acetic acid. After air-drying, 10 mM Tris solution (pH 7.5) was added to dissolve the protein-bound dye. Cell survival was assessed by optical density (OD) determination at 510 nm using a microplate reader.

For the *in vitro* scratch assay, Ad-MSCs were seeded into 6-well microplates and grown in complete medium to a confluent monolayer. Analogously, HaCaT cells (50,000 cells/well) were seeded into 12-well plates in DMEM supplemented with 10% FBS and allowed to adhere for 24 h. Cell monolayers were carefully scratched with a sterile pipette tip, washed twice with phosphate buffer saline (PBS) and incubated at 37 °C with a medium containing 1% FBS (for HaCaT cells) or 0.25% BSA (for Ad-MSCs) with or without the hydrogels. Reference points near the scratch were marked to guarantee the same area of image acquisition. Images of wound gap were taken at different time points by a digital camera coupled to the microscope and percentage of closure was calculated with IMAGE J (NIH, USA). These experiments were repeated at least three times.

2.6. In vivo *wound healing studies*

A full-thickness excision wound model was used to monitor wound closure. Male Wistar albino rats weighing 300–350 g (Harlan, Italy) were housed singly in Plexiglas cage for one week at temperature of 22 ± 1 °C, with alternate cycle of 12 h of light and 12 h of dark. All animals received food and water ad libitum throughout the experimental period. All manipulations were performed using aseptic techniques. This study was carried out in strict accordance with the Institutional Guidelines and complied with the Italian D.L. no. 116 of January 27, 1992 of Ministero della Salute and associated guidelines in the European Communities Council Directive of November 24, 1986 (86/609/ECC).

All the animals were anesthetized with ketamine hydrochloride (100 mg/kg body weight) and xylazine (5 mg/kg) by intraperitoneal administration, and the dorsal hair was shaved using a shaving machine. The dorsal region was chosen to avoid animal access to their own wound and animals were housed one per box to prevent cross-access to the lesions. The surgical area was disinfected with Betadine R 10%. A full-thickness wound with a diameter of 2.5 cm was excised from the back of the rats using sterile scissors at the depth of loose subcutaneous tissues. Hemostasis was obtained by direct pressure using sterile gauze. Before hydrogel application the wound was moistened with 300 μL of saline. Animals ($n = 6$) were divided into two groups and wounds were treated with a single application of hydrogels (ALG, ALG/HA20). Wound site was finally closed with non-occlusive Tegaderm™ (3M, USA). At days 0, 1, 5 wound size was measured using Image J software (NIH, USA). The rate of wound closure that represents the percentage of wound reduction from the original wound size was calculated using the following formula: [wound area day 0 − wound area (day 1 or 5)]/wound area day 0 × 100. Values are expressed as percentage of the healed wounds ± SD.

2.7. Statistical analysis

Error bars represent mean ± SD of biological replicates. Statistical comparisons were made by one-way ANOVA followed by Bonferroni's test for multiple comparisons. $^{*}p < 0.05$; $^{**}p < 0.01$; $^{***,\#\#\#}p < 0.001$. $p > 0.05$ was considered not statistically significant.

3. Results and discussion

3.1. Internal gelation of ALG and ALG/HA hydrogels

One of the aims of this study was to formulate compact hydrogels able to remain intact after gelation and with sufficient strength to be easily positioned on the wound bed during the dressing change.

Although cross-linking of ALG via divalent cations is a simple strategy to produce hydrogels, their stiffness strongly depends on G/M ratio. In particular, structural integrity and mechanical properties are highly related to crosslink of G-blocks that form more highly ordered regions when ionically interacting with divalent cations (Smidsrød & Skjåk-Bræk, 1990). In general hydrogel stiffness varies in the order MG < MM < GG while elasticity follows an opposite trend. The M/G ratio and the number of repeated G and M units in a single segment can thereby affect the gelation process and, in turn, hydrogel physical structure (strength and porosity).

M/G ratio of the raw ALG employed in this study as evaluated by ^{1}H NMR was 1.54 (Supplementary material S1), a value in line with those previously reported for ALG produced by *Macrocystis pyrifera* (Moe, Draget, Skjåk-Bræk, & Smidsrød, 1995). While not fully indicated to give hydrogels with suitable mechanical properties, we attempted to control ALG gelation rate, also in the presence of HA chains, to obtain hydrogels fulfilling requirements of a wound dressing (Draget et al., 1990).

As a first step of the study, we tried to evaluate if the addition of HA could modify gelation properties of ALG, which is an important variable in hydrogel formulation. Previous studies have shown that a fast gelation can lead to a poorly homogeneous gel structure (Kuo & Ma, 2001). To determine the liquid-to-solid transition point (i.e., the so called "critical gel" state) samples were subjected to a continuous series of frequency sweeps (in the range 0.03–100 rad/s) and the gel time was determined rheologically as the instant where G′ and G″ are parallel to each other or equivalently where the loss

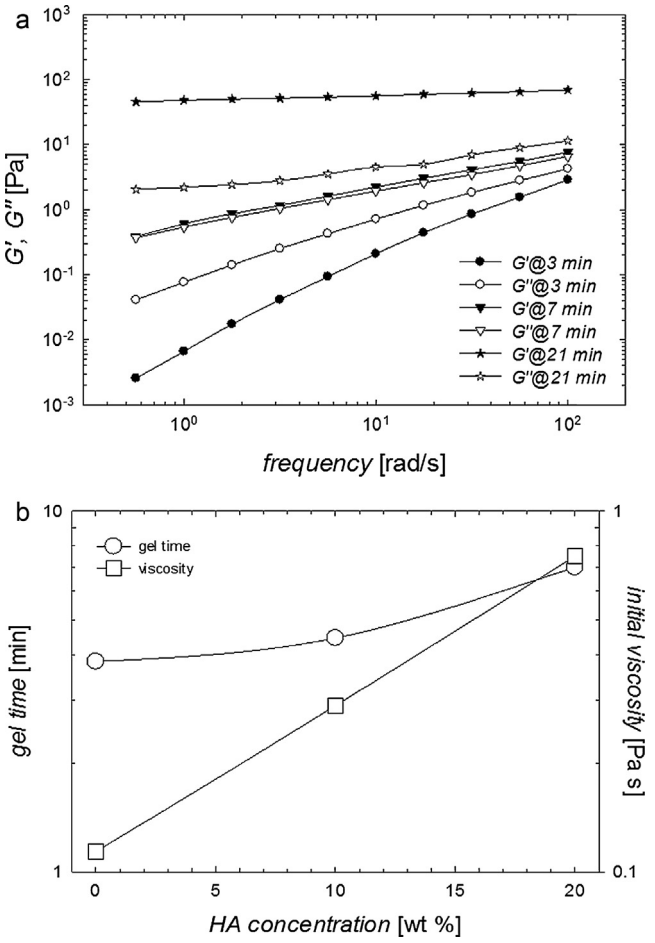

Fig. 1. Rheological characterization of gelation process. (A) Viscoelastic moduli as a function of frequency for ALG/HA20 at different times after beginning of internal gelation process. (B) Gelation time and initial viscosity of ALG/HA solutions at different HA concentration.

phase angle is frequency independent (Chambon et al., 1987). The time-evolution of viscoelastic moduli for the ALG/HA20 system is reported in Fig. 1A (ALG solution containing a different amount of HA showed similar behaviors and consequently the corresponding data are not shown). Inspection of Fig. 1A informs us that for times shorter than 3 min the sample shows a liquid-like behavior with a viscous modulus (G'') higher than the elastic component (G') and a strong dependency upon frequency. At 7 min, the relaxation spectrum of the sample showed a critical gel behavior with a power-law dynamics and G' and G'' parallel to one another. At this condition the material behaves not as a liquid (as its spectrum results in an infinite shear viscosity) and not yet as a solid (as its equilibrium modulus is null). At times longer than 7 min (see for instance the curves referring to 21 min in Fig. 1A), the system showed a solid-like behavior with the elastic modulus much higher than the viscous component and a scarcely pronounced dependency upon frequency.

Gelation times, measured with the method of Chambon and Winter (1987) described above, were plotted as a function of HA content in Fig. 1B; on the same figure the initial viscosity of the solutions was also plotted as a function of HA content. Both gelation time and initial viscosity of solutions show a monotonic increasing behavior as a function of HA content, the two phenomena being clearly correlated. Indeed, the ALG gelation process is controlled by the mobility of G-blocks and calcium ions that interact to from cross-links and give rise to an "egg box" structure. In this view an increased viscosity of the initial solution results in a decreased ALG chains and calcium ions mobility, due to slower diffusion, and, consequently, in a longer gelation time.

At the end of the gelation process, the resulting hydrogels had elastic shear moduli (G') of about 1 kPa, viscous shear moduli (G'') about one order of magnitude smaller, and for both a weak frequency dependency. Furthermore, while viscoelastic properties of initial solution and gelation time do strongly depend upon HA content (with higher contents corresponding to more elastic systems), after the gelation has completed all the systems have similar behavior and similar moduli. Compressive tests performed in quasi-static conditions (data not shown) confirmed these findings with all samples showing similar (strain-hardening) behavior, stress at 10% deformation ranging between 200 and 300 Pa and compression moduli in the order of few kPa (Nunamaker, Otto, & Kipke, 2011; Zhang et al., 2008). These observations suggest that, although the presence of HA does significantly slow down gelation kinetics, the concentration of cross-links reached at the end of gelation is scarcely affected by HA.

Uniform and transparent ALG hydrogels were obtained at calcium carbonate/GDL molar ratio of 2 (Fig. 2A), which guarantees also that pH of the final hydrogel is close to neutrality (Draget et al., 1989). SEM of ALG/HA hydrogels after freeze drying (Fig. 2B) showed randomly distributed interconnected pores in the size range 50–150 μm. The investigated hydrogels showed sufficient strength to be handled, cut or packed without experiencing any difficulty.

3.2. Hydrogel homogeneity

Amid the large number of factors affecting ALG gelation time (Alexander, Murphy, Gallagher, Farrell, & Taggart, 2012), concentration of calcium carbonate in the polymer solution is of utmost importance since it controls availability of soluble calcium ions available for crosslinking. On the other hand, calcium carbonate is dispersed in a polymer solution and can progressively accumulate at the bottom of recipient giving non-homogeneous cross-linking. Structural uniformity is crucial for biomedical applications not only from a drug delivery point of view to achieve uniform distribution of the drug in the matrix, but especially to get adequate material properties. To evaluate the homogeneity of hydrogels made with $CaCO_3$–GDL, cylindrical gels with varying compositions were prepared, sliced along the vertical axis and dry/wet ratio evaluated. Comparable homogeneity profiles of ALG gels at different HA concentrations indicated that the presence of HA did not affect gel homogeneity in the concentration range studied (Fig. 3).

3.3. Cross-linking degree

The swelling behavior of ALG hydrogels is a function of crosslink density, ALG concentration and ALG chemical composition (Kuo & Ma, 2008). During the internal gelation, calcium ions are released directly inside the ALG solution and, for this reason, their diffusion in the solution is essential to control cross-linking degree and in turn swelling. To determine whether hydrogels composition affected cross-linking degree, the effect of calcium chloride addition on equilibrium swelling (7 days) of different hydrogels was investigated (Fig. 4).

It was found that, independently of the presence of HA, all hydrogels gave a similar swelling behavior with a shrinking that directly depends from the calcium concentration in the medium. The W/W_0 ratio was similar for all the formulation, in agreement with mechanical data, suggesting that the presence of HA had a minimal influence on the crosslinking degree.

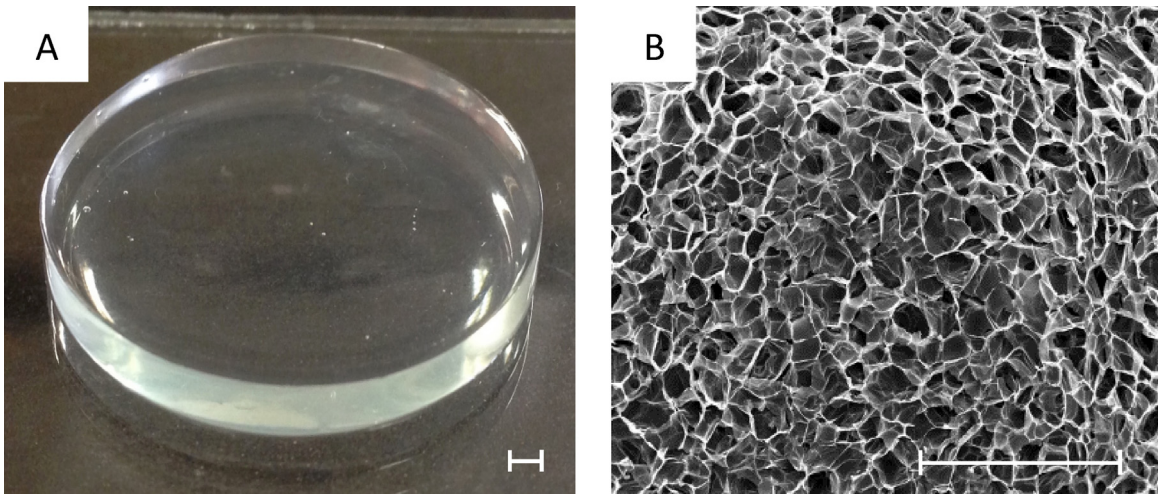

Fig. 2. ALG/HA20 hydrogel after completion of internal gelation process (A) and after freeze drying (B). Scale bar = 1 mm.

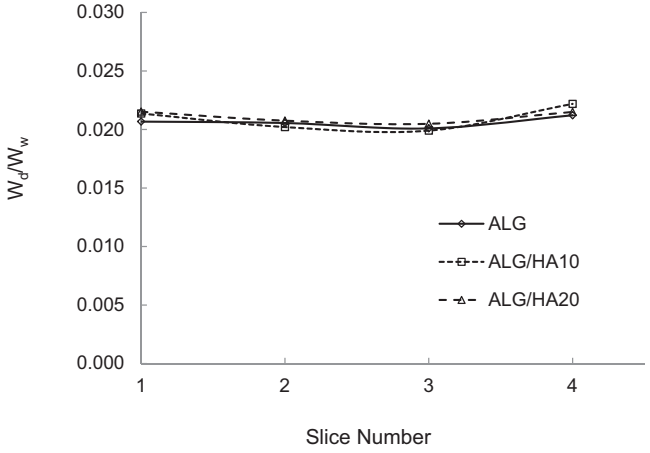

Fig. 3. Homogeneity of ALG hydrogels prepared with different HA content. Slices were numbered 1–4, from top to bottom and dry (W_d) to wet (W_w) weight ratio measured.

3.4. Biological evaluation of ALG and ALG/HA hydrogels

In order to evaluate the *in vitro* toxicity of hydrogels, Ad-MSCs previously isolated from subcutaneous adipose tissue biopsies (D'Esposito et al., 2012) were tested. Indeed, *in vitro* predictive toxicological assays based on human stem cells and their derivatives offer significant advantages over animal models largely due to improved relevance and greater versatility. The use of human stem cell systems might dramatically increase the ability to predict toxic responses in humans while decreasing the need for extensive toxicity tests in animals (Liu, Deng, Liu, Gong, & Deng, 2013). Ad-MSCs viability was investigated using a transwell system where the upper chamber contained the hydrogels, while the lower chamber was loaded with a cell suspension in DMEM F12 (1:1) 10% FBS. Sulforhodamine assay revealed that Ad-MSC viability in the presence of ALG and ALG/HA hydrogels was comparable to that achieved in complete medium (Fig. 5) indicating that combination of ALG and HA neither represents a toxic environment for Ad-MSCs nor induces cell proliferation.

The excellent biocompatibility of hydrogels encouraged us to investigate whether ALG and ALG/HA hydrogels could affect cell motility in an *in vitro* scratch assay. On the basis of mechanical properties and toxicity data, ALG/HA20 (highest HA content) was selected for further experiments.

Since HA exerts profound effects on MSC residing in HA-rich microenvironments that maintain cells in a quiescent state, HA

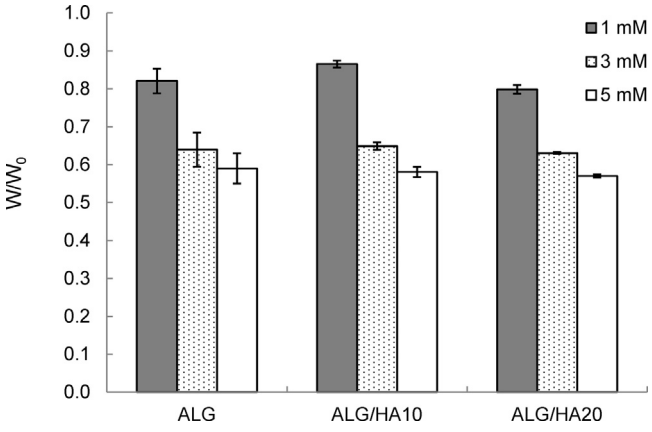

Fig. 4. Equilibrium swelling of ALG hydrogels immersed for 7 days in water containing different amounts of calcium chloride. Data are reports as ratio between wet weight at designated time (W) and initial wet weight (W_0).

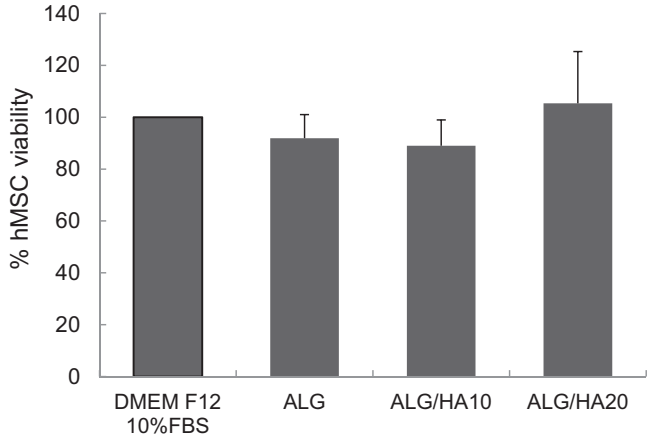

Fig. 5. Effect of ALG and ALG/HA hydrogels on Ad-MSCs viability. ALG or ALG/HA hydrogels (ALG/HA10 – ALG/HA20) have been added in the upper chamber of the transwell in DMEM F12 (1:1) 10% FBS. Upon 24 h, cell viability has been determined. The results have been reported as percentage of viable cells compared with cells incubated in DMEM F12 (1:1) 10% FBS in the absence of hydrogels (considered as 100% viable cells). Bars represent the mean ± SD of triplicate determination in three independent experiments.

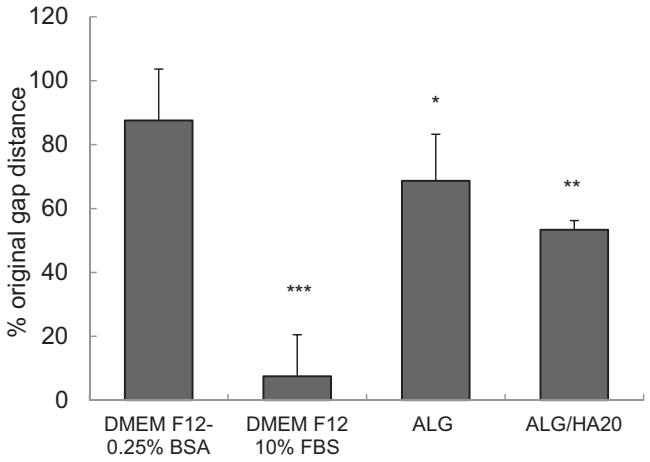

Fig. 6. Effect of ALG and ALG/HA20 hydrogels on Ad-MSCs motility. Confluent monolayers of Ad-MSCs have been scratched, washed twice with PBS and incubated at 37 °C in the presence of ALG or ALG/HA (ALG/HA20) hydrogels in DMEM F12 (1:1) 0.25% BSA. The results are reported as percentage of gap distance at 24 h compared with time 0. Bars represent the mean ± SD of triplicate determination in three independent experiments. Statistically significant differences respect to cells in DMEM F12 (1:1) 0.25% BSA (*$p < 0.05$; **$p < 0.01$; ***$p < 0.001$).

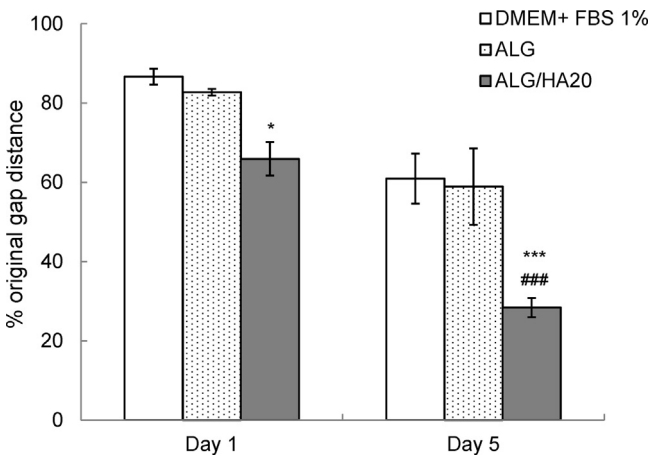

Fig. 7. Effect of ALG and ALG/HA20 hydrogels on HaCaT motility. Confluent monolayers of HaCaT have been scratched, washed twice with PBS and incubated at 37 °C in the presence of ALG or ALG/HA20 hydrogels in DMEM with 1% FBS. The results have been reported as percentage of gap distance at day 1 and day 5 compared with the time 0. Data are shown as mean ± SEM of triplicate determination in three independent experiments. ***$p < 0.001$, and *$p < 0.05$ vs. DMEM with 1% FBS; ###$p < 0.001$ vs. ALG.

role on migration of stem cell populations is expected to be critical for the preparation of tissue regeneration and for the recruitment of MSC into wound sites (Zhu et al., 2006). Furthermore, recent evidences point at Ad-MSCs as a promising cell-based treatment option to meet the challenges of impaired skin wound healing such as diabetic foot ulcers (Hassan, Greiser, & Wang, 2014). Ad-MSCs were scratched and incubated with ALG and ALG/HA20 hydrogels for 24 h in medium without serum supplementation (DMEM F12 −0.25% BSA). As shown in Fig. 6, serum induced an almost complete filling of gap. Even in absence of serum, ALG/HA20 hydrogel significantly promoted gap closure as compared to serum-free medium ($p < 0.01$, respectively).

The same experiment was replicated using confluent monolayers of HaCaT which provide a reliable *in vitro* model of re-epithelialization phase in wound healing (Raja Sivamani et al., 2007). In analogy to Ad-MSC, hydrogels did not interfere with HaCaT cell viability (data not shown). Confluent monolayers of HaCaT were scratched and incubated with ALG and ALG/HA hydrogels in medium with 1% FBS. Images were taken at 0, day 1 and day 5 after scratch. As shown in Fig. 7, ALG and ALG/HA20 hydrogels significantly promoted reduction of gap distance at day 1 as compared to medium with 1% FBS while ALG hydrogel did not. This effect was more significant at day 5 ($p < 0.001$) and most likely due to increased cell motility, since the experiments were carried out with low serum concentration in order to reduce cell proliferation. As reviewed recently, current evidences suggest HA/CD44-mediated activation of different signaling pathways leads to the regulation of keratinocyte activities and following epidermal functions

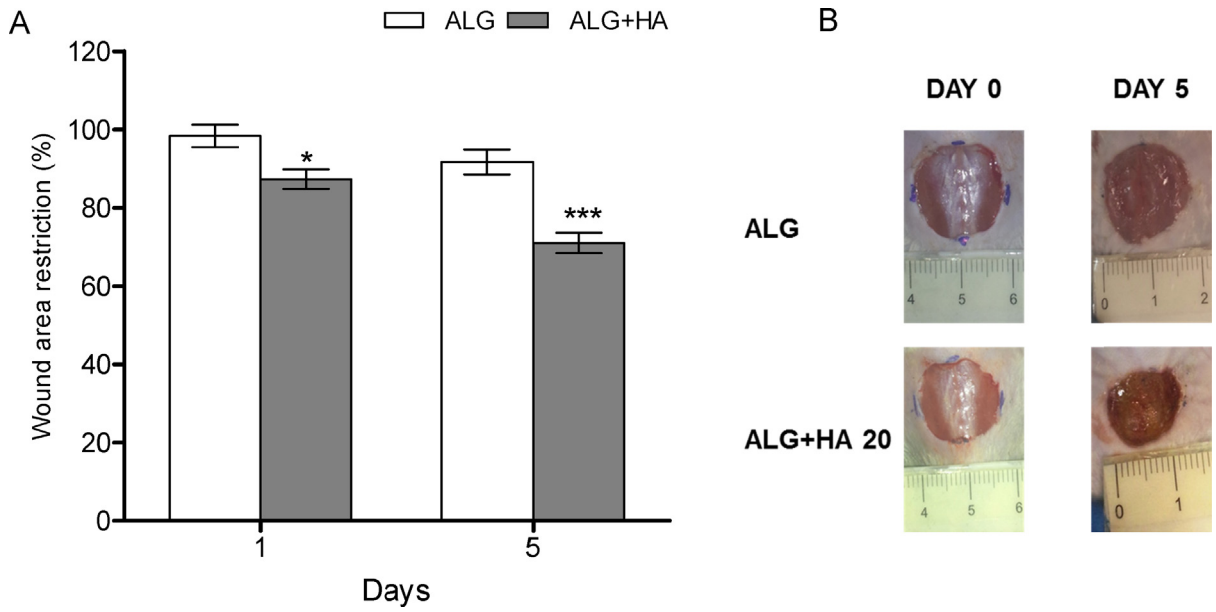

Fig. 8. Effects of ALG hydrogels on healing process in a rat model of excised wound. A full-thickness wound was excised from the back of the rats ($n = 6$) using sterile scissors and left open. Wounds were treated with hydrogels (ALG, ALG/HA20) and closed with Tegaderm™. (A) Wound area restriction on day 1 and 5 as compared to day 0 is reported. *$p < 0.05$; ***$p < 0.001$ vs. ALG hydrogel.

(Bourguignon, 2014). Thus, the improved migration of HaCaT can be reasonably attributed to HA binding to the cell surface receptor CD44, which controls migration of keratinocyte collecting at the wound edge in the wound site (Chen & Abatangelo, 1999).

These data support the hypothesis that ALG/HA hydrogels could potentiate re-epithalization of the wounded site by stimulation of Ad-MSC and HaCaT motility and may have a potential interest in tissue engineering procedures.

Since data obtained from scratch assay cannot mimic the complexity of events that occur during the wound healing process, *in vitro* data were corroborated on the full excision wound model in rats. ALG and ALG/HA hydrogels were applied on rat backs and the capacity of hydrogels to restrict wound area was evaluated. As reported in Fig. 8, ALG/HA20 induced a significant reduction of wound extension after 1 and 5 days from application ($p < 0.05$ and $p < 0.001$, respectively) whereas, no evident effect was detectable using ALG alone. Enhanced tissue repair ability of ALG/HA hydrogels in the early phase of inflammatory response can be reasonably ascribed to the recapitulation of induction signals exerted by HA. Indeed, HA naturally interacts with signaling receptors (primarily CD44) to initiate inflammatory response, to maintain structural cell integrity and to promote recovery from tissue injury (Zhu et al., 2006). Furthermore, a possible activity of HA on peroxisome proliferator-activated receptors (PPARs) during wound healing cannot be excluded (Fronza et al., 2014). The formation of a highly hydrated HA-rich matrix can be supposed to facilitate cell migration into the provisional wound matrix fostering proliferation and in turn regeneration process (Abatangelo, Cortivo, Martelli, & Vecchia, 1982). Although wound contraction is the primary mechanism underlying healing process of closure in the murine model adopted (Pastar et al., 2014), re-epithelialization of the wound site, which is prevalent in human skin, and suggested by *in vitro* results, can well take place and contribute to wound closure as observed elsewhere (Liu, Petreaca, Yao, & Martins-Green, 2009).

4. Conclusions

Hydrogels based on ALG and HA, a polysaccharide with a crucial role in wound healing process, have been successfully produced and characterized. The internal gelation method gave hydrogels with good handling characteristics and suitable mechanical properties as wound dressing. Although the presence of HA affected ALG gelation time, its limited influence on the overall properties of hydrogels was found. *In vitro* scratch assay in different cell lines highlighted that HA incorporation into ALG hydrogels promoted cell migration without affecting viability. Finally, a significant reduction of wound area in an excision wound model in rats was found for the hydrogel with HA. Taken together, these results demonstrate that integration of HA in an ionically crosslinked ALG matrix can be a versatile strategy to promote wound healing process easy to translate in a clinical setting. Furthermore, it is anticipated that ALG/HA hydrogels can also act as a potential platform to deliver bioactive compounds directly in the wound bed.

Acknowledgements

The authors wish to thank Prof. Alfonso Carotenuto and Dr. Antonio Limatola for NMR analysis of alginates and Dr Domenico Liguoro (IEOS, CNR) for technical help with cell cultures. The financial support of Italian Ministry of University and Research (PRIN 2010H834LS) is gratefully acknowledged.

Appendix A. Supplementary data

Supplementary data associated with this article can be found, in the online version, at http://dx.doi.org/10.1016/j.carbpol.2015.05.081

References

Abatangelo, G., Cortivo, R., Martelli, M., & Vecchia, P. (1982). Cell detachment mediated by hyaluronic acid. *Experimental Cell Research*, *137*, 73–78.
Alexander, B. R., Murphy, K. E., Gallagher, J., Farrell, G. F., & Taggart, G. (2012). Gelation time, homogeneity, and rupture testing of alginate-calcium carbonate-hydrogen peroxide gels for use as wound dressings. *Journal of Biomedical Materials Research Part B – Applied Biomaterials*, *100B*, 425–431.
Boateng, J. S., Matthews, K. H., Stevens, H. N., & Eccleston, G. M. (2008). Wound healing dressings and drug delivery systems: A review. *Journal of Pharmaceutical Sciences*, *97*, 2892–2923.
Bourguignon, L. Y. W. (2014). Matrix hyaluronan-activated CD44 signaling promotes keratinocyte activities and improves abnormal epidermal functions. *American Journal of Pathology*, *184*, 1912–1919.
Braccini, I., & Perez, S. (2001). Molecular basis of C(2+)-induced gelation in alginates and pectins: The egg-box model revisited. *Biomacromolecules*, *2*, 1089–1096.
Chambon, F., & Winter, H. H. (1987). Linear viscoelasticity at the gel point of a crosslinking PDMS with imbalanced stoichiometry. *Journal of Rheology*, *31*, 683–697.
Chen, W. Y. J., & Abatangelo, G. (1999). Functions of hyaluronan in wound repair. *Wound Repair and Regeneration*, *7*, 79–89.
Chiba, K., Kawakami, K., & Tohyama, K. (1998). Simultaneous evaluation of cell viability by neutral red, MTT and crystal violet staining assays of the same cells. *Toxicology In Vitro*, *12*, 251–258.
D'Esposito, V., Passaretti, F., Hammarstedt, A., Liguoro, D., Terracciano, D., Molea, G., et al. (2012). Adipocyte-released insulin-like growth factor-1 is regulated by glucose and fatty acids and controls breast cancer cell growth in vitro. *Diabetologia*, *55*, 2811–2822.
David-Raoudi, M., Tranchepain, F., Deschrevel, B., Vincent, J. C., Bogdanowicz, P., Boumediene, K., et al. (2008). Differential effects of hyaluronan and its fragments on fibroblasts: Relation to wound healing. *Wound Repair Regeneration*, *16*, 274–287.
Dicker, K. T., Gurski, L. A., Pradhan-Bhatt, S., Witt, R. L., Farach-Carson, M. C., & Jia, X. Q. (2014). Hyaluronan: A simple polysaccharide with diverse biological functions. *Acta Biomaterialia*, *10*, 1558–1570.
Draget, K. I., Ostgaard, K., & Smidsrod, O. (1989). Alginate-based solid media for plant-tissue culture. *Applied Microbiology and Biotechnology*, *31*, 79–83.
Draget, K. I., Ostgaard, K., & Smidsrod, O. (1990). Homogeneous alginate gels – A technical approach. *Carbohydrate Polymers*, *14*, 159–178.
Draget, K. I., Simensen, M. K., Onsoyen, E., & Smidsrod, O. (1993). Gel strength 514 of Ca-limited alginate gels made in situ. *Hydrobiologia*, *260–261*, 563–565.
Foschi, D., Castoldi, L., Radaelli, E., Abelli, P., Calderini, G., Rastrelli, A., et al. (1990). Hyaluronic acid prevents oxygen free-radical damage to granulation tissue: A study in rats. *International Journal Tissue Reactions*, *12*, 333–339.
Frenkel, J. S. (2012). The role of hyaluronan in wound healing. *International Wound Journal*, *11*, 159–163.
Fronza, M., Caetano, G. F., Leite, M. N., Bitencourt, C. S., Paula-Silva, F. W. G., Andrade, T. A. M., et al. (2014). Hyaluronidase modulates inflammatory response and accelerates the cutaneous wound healing. *PLOS ONE*, *9*, e112297.
Gilchrist, T., & Martin, A. M. (1983). Wound treatment with Sorbsan – An alginate fibre dressing. *Biomaterials*, *4*, 317–320.
Grant, G. T., Morris, E. R., Rees, D. A., Smith, P. J. C., & Thom, D. (1973). Biological interactions between polysaccharides and divalent cations: The egg-box model. *FEBS Letters*, *32*, 195–198.
Gurtner, G. C., Werner, S., Barrandon, Y., & Longaker, M. T. (2008). Wound repair and regeneration. *Nature*, *453*, 314–321.
Hassan, W. U., Greiser, U., & Wang, W. (2014). Role of adipose-derived stem cells in wound healing. *Wound Repair and Regeneration*, *22*, 313–325.
King, S. R., Hickerson, W. L., & Proctor, K. G. (1991). Beneficial actions of exogenous hyaluronic acid on wound healing. *Surgery*, *109*, 76–84.
Kocaoemer, A., Kern, S., Kluter, H., & Bieback, K. (2007). Human AB serum and thrombin-activated platelet-rich plasma are suitable alternatives to fetal calf serum for the expansion of mesenchymal stem cells from adipose tissue. *Stem Cells*, *25*, 1270–1278.
Kuo, C. K., & Ma, P. X. (2001). Ionically crosslinked alginate hydrogels as scaffolds for tissue engineering: Part 1. Structure, gelation rate and mechanical properties. *Biomaterials*, *22*, 511–521.
Kuo, C. K., & Ma, P. X. (2008). Maintaining dimensions and mechanical properties of ionically crosslinked alginate hydrogel scaffolds in vitro. *Journal of Biomedical Materials Research Part A*, *84A*, 899–907.
Lee, K. Y., & Mooney, D. J. (2012). Alginate: Properties and biomedical applications. *Progress in Polymer Science*, *37*, 106–126.
Liu, W. W., Deng, Y. G., Liu, Y., Gong, W. R., & Deng, W. B. (2013). Stem cell models for drug discovery and toxicology studies. *Journal of Biochemical and Molecular Toxicology*, *27*, 17–27.
Liu, Y., Petreaca, M., Yao, M., & Martins-Green, M. (2009). Cell and molecular mechanisms of keratinocyte function stimulated by insulin during wound healing. *BMC Cell Biology*, *10*, 1.

Moe, S. T., Draget, K. I., Skjåk-Bræk, G., & Smidsrød, O. (1995). Alginates. In A. M. Stephen (Ed.), *Food polysaccharides and their applications* (pp. 245–286). New York: Marcel Dekker.

Morch, Y. A., Donati, I., Strand, B. L., & Skjak-Braek, G. (2006). Effect of Ca^{2+}, Ba^{2+}, and Sr^{2+} on alginate microbeads. *Biomacromolecules*, *7*, 1471–1480.

Nunamaker, E. A., Otto, K. J., & Kipke, D. R. (2011). Investigation of the material properties of alginate for the development of hydrogel repair of dura mater. *Journal of the Mechanical Behavior of Biomedical Materials*, *4*, 16–33.

Pastar, I., Stojadinovic, O., Yin, N. C., Ramirez, H., Nusbaum, A. G., Sawaya, A., et al. (2014). Epithelialization in wound healing: A comprehensive review. *Advances in Wound Care (New Rochelle)*, *3*, 445–464.

Peppas, N. A., Huang, Y., Torres-Lugo, M., Ward, J. H., & Zhang, J. (2000). Physicochemical foundations and structural design of hydrogels in medicine and biology. *Annual Review of Biomedical Engineering*, *2*, 9–29.

Petrey, A. C., & de la Motte, C. A. (2014). Hyaluronan, a crucial regulator of inflammation. *Frontiers in Immunology*, *5*, 1–13.

Queen, D., Orsted, H., Sanada, H., & Sussman, G. (2004). A dressing history. *International Wound Journal*, *1*, 59–77.

Raja Sivamani, K., Garcia, M. S., & Isseroff, R. R. (2007). Wound re-epithelialization: Modulating keratinocyte migration in wound healing. *Frontiers in Bioscience*, *12*, 2849–2868.

Singer, A. J., & Clark, R. A. (1999). Cutaneous wound healing. *The New England Journal of Medicine*, *341*, 738–746.

Skjåk-Bræk, G., Grasdalen, H., & Smidsrød, O. (1989). Inhomogeneous polysaccharide ionic gels. *Carbohydrate Polymers*, *10*, 31–54.

Slaughter, B. V., Khurshid, S. S., Fisher, O. Z., Khademhosseini, A., & Peppas, N. A. (2009). Hydrogels in Regenerative Medicine. *Advanced Materials*, *21*, 3307–3329.

Smidsrød, O., & Skjåk-Bræk, G. (1990). Alginate as immobilization matrix for cells. *Trends in Biotechnology*, *8*, 71–78.

Toole, B. P. (2004). Hyaluronan: From extracellular glue to pericellular cue. *Nature Reviews Cancer*, *4*, 528–539.

Trabucchi, E., Pallotta, S., Morini, M., Corsi, F., Franceschini, R., Casiraghi, A., et al. (2002). Low molecular weight hyaluronic acid prevents oxygen free radical damage to granulation tissue during wound healing. *International Journal of Tissue Reactions*, *24*, 65–71.

Voigt, J., & Driver, V. R. (2012). Hyaluronic acid derivatives and their healing effect on burns, epithelial surgical wounds, and chronic wounds: A systematic review and meta-analysis of randomized controlled trials. *Wound Repair and Regeneration*, *20*, 317–331.

West, D. C., Hampson, I. N., Arnold, F., & Kumar, S. (1985). Angiogenesis induced by degradation products of hyaluronic acid. *Science*, *228*, 1324–1326.

Zhang, L. F., Yang, D. J., Chen, H. C., Sun, R., Xu, L., Xiong, Z. C., et al. (2008). An ionically crosslinked hydrogel containing vancomycin coating on a porous scaffold for drug delivery and cell culture. *International Journal of Pharmaceutics*, *353*, 74–87.

Zhu, H., Mitsuhashi, N., Klein, A., Barsky, L. W., Weinberg, K., Barr, M. L., et al. (2006). The role of the hyaluronan receptor CD44 in mesenchymal stem cell migration in the extracellular matrix. *Stem Cells*, *24*, 928–935.